[redacted]

AEC Category: HEALTH AND SAFETY

[redacted]

CEX-61.1 (Prelim.)

CIVIL EFFECTS STUDY

GAMMA RADIATION AT THE AIR-GROUND INTERFACE

Keran O'Brien and James E. McLaughlin, Jr.

Issuance Date: May 29, 1963

CIVIL EFFECTS TEST OPERATIONS
U.S. ATOMIC ENERGY COMMISSION

NOTICE

This report is published in the interest of providing information which may prove of value to the reader in his study of effects data derived principally from nuclear weapons tests and from experiments designed to duplicate various characteristics of nuclear weapons.

This document is based on information available at the time of preparation which may have subsequently been expanded and re-evaluated. Also, in preparing this report for publication, some classified material may have been removed. Users are cautioned to avoid interpretations and conclusions based on unknown or incomplete data.

USAEC Division of Technical Information Extension, Oak Ridge, Tennessee

Preliminary Report

GAMMA RADIATION AT THE AIR-GROUND INTERFACE

By

Keran O'Brien

and

James E. McLaughlin, Jr.

Approved by: L. J. DEAL
Acting Chief
Civil Effects Branch

Health and Safety Laboratory
New York Operations Office

October 1962

ABSTRACT

Measurements were made at the Nevada Test Site of dose rates produced by two large gamma-ray sources positioned in a level, clear area. The distance between each source in turn and the detectors was varied from about 10 m to almost 1 km, and the height of the detectors was increased from 0 to 148 m, or roughly one mean free path. The data obtained with several ionization chambers are presented and discussed. These data are to be used in determining the effect of the air–ground interface on gamma-ray dose rates produced by point and distributed sources on the ground.

ACKNOWLEDGMENTS

The authors are indebted to their associates, Robert Sanna, Stephen Samson, William Condon, Sam Rothenberg, and Stephen Lanes, whose efforts were essential to the conduct of the experiment, and to Pauline Castellani and Gladys Lopez for their help in preparing the manuscript.

Others who contributed greatly in terms of support and encouragement are

Wayne Lowder, Jack Dowdall, and Noel Klores, and several members of the Instrument Division, Health and Safety Laboratory

L. J. Deal and John Williamson, Civil Effects Test Operations

Zolin Burson, John Elmgren, Patrick Murphy, and Robert Summers, Edgerton, Germeshausen & Grier, Inc.

F. Woodworth, Colin Shanks, and Byron Bollé of the various Nevada Test Site support functions

CONTENTS

ILLUSTRATIONS

ILLUSTRATIONS (Continued)

CHAPTER 3 PRESENTATION OF DATA

TABLES

CHAPTER 3 PRESENTATION OF DATA

Chapter 1

INTRODUCTION

1.1 BACKGROUND

Until recently, for a calculation of the dose rates produced by gamma-ray sources on the earth's surface, it has been considered sufficient to assume that the medium in which the gamma-ray intensities are measured is infinite in extent and homogeneous in composition. In this report calculations of this type are referred to as homogeneous-theory calculations.

Many of the attempts to interpret dose rates from fallout emitters have proceeded from a point kernel obtained from homogeneous theory. Obviously errors in the kernel obtained in this manner will also appear in dose-rate calculations of the integral source array. In evaluating the departure of the actual dose rates from those calculated from homogeneous theory, one finds that attention is centered on the interface effect.

The calculations of Berger[1] put into proper perspective the problem of gamma-ray transport at the interface near two half spaces differing greatly in density. Before Berger's calculations few calculations made any attempt to take into account the abrupt discontinuity between the earth and the air. Hence inferences relating dose rates in air to radioactivity deposited by fallout have been opened to question.

Homogeneous calculations have been used in various Health and Safety Laboratory (HASL) projects to estimate the effects of fallout from the worldwide distribution of the debris of nuclear devices[2-4] as well as in the well-known book *The Effects of Nuclear Weapons*.[5]

The adequacy of this conventional approach was questioned as long ago as 1951, as a result of the measurements of gamma-ray dose rates from fallout over the center of a cleared area during the Jangle weapons test series.[6] Measured dose rates differed from those calculated by a factor of about 3 and increased rapidly with height (instead of decreasing), a behavior confirmed by Graveson[7] during the Redwing series in 1956.

In discussing the correspondence between homogeneous-theory calculations and experimental results, many authors, observing the vast difference between the theoretical plane of the integration and the earth's surface, attributed the disagreement to the roughness and irregularities of the ground.[6,7]

This hypothesis gained wide currency, despite the fact that there was no mathematical technique for handling surface-roughness effects. Kleinecke[8] pointed out that the effects hitherto associated with ground roughness were probably a result of the fact that the gamma rays are emitted by fallout lying on the air–ground interface and that the effect of this interface on gamma-ray transport in its vicinity was ignored because it was unknown.

Berger's calculations,[1] by means of the Monte Carlo technique, were made of the energy dissipation by gamma rays in water divided into two half spaces by a plane interface. The two regions were similar in composition, but greatly different in density. The calculations were for a 1.28-Mev isotropic gamma-ray point source at or near the bounding plane, and the results were expressed in terms of correction factors which compared the energy dissipation to that which would prevail if the source–detector distance were the same but were in an infinite, homogeneous medium.

Berger's results were experimentally confirmed by Titus,[9] who used Co^{60} gamma rays in an iron–steel-wool medium. Further work was done by Clifford et al.,[10] who used Cs^{137} gamma rays in an air–clay medium, polystyrene-foam–concrete medium, and a polystyrene-foam–lead medium. These values have received some computational support in Kleinecke's work.[8]

In summary, then, the calculations of gamma-ray dose rates from fallout have been based on the assumption that the surface of the earth, if it were ideally smooth, need not be taken into account. On the other hand, it has been recognized for some years that the plane integral of a point kernel obtained for an infinite homogeneous medium does not adequately represent reality.

1.2 OBJECTIVE

The calculations of Berger showed that the presence of a density interface in the vicinity of a gamma-ray source would have a pronounced effect on the dose rate. We felt it quite probable that some of the observed anomalies in the transport of fallout gamma rays could be attributed to this interface effect.

Experimental work done thus far[9,10] is of great value in supporting Berger's calculations and in indicating the presence of a dependence on source energy. The present gamma-ray experiment was conducted as an extension of this earlier experimental work. The results should be useful in analyzing the dose rates produced by sources distributed on or near the earth's surface.

REFERENCES

1. M. J. Berger, Calculation Of Energy Dissipation by γ-Radiation Near The Interface Between Two Media, *J. Appl. Phys.*, 28: 1502–1508(December 1957).
2. N. A. Hallden and J. H. Harley, *Method of Calculating Infinity Gamma Dose from Beta Measurements on Gummed Film*, USAEC Report NYO-4859, New York Operations Office, Apr. 15, 1957.
3. J. H. Harley, N. A. Hallden, and L. D. Y. Ong, *Summary of Gummed Film Results Through December 1959*, USAEC Report HASL-93, New York Operations Office, Sept. 5, 1960.
4. W. R. Collins, Jr., G. A. Welford, and R. S. Morse, Fallout from 1957 and 1958 Nuclear Test Series, *Science*, 134: 980–984(Oct. 6, 1961).
5. S. Glasstone (Ed.), *The Effects of Nuclear Weapons*, rev. ed., Chapter IX, U. S. Government Printing Office, Washington 25, D. C., April 1962.
6. A. J. Breslin and L. R. Solon, *Fallout Countermeasures For AEC Facilities*, USAEC Report NYO-4682-A, New York Operations Office, December 1955.
7. R. T. Graveson, *Radiation Protection Within a Standard Housing Structure*, USAEC Report NYO-4714, New York Operations Office, November 1956.
8. D. C. Kleinecke, The Effect of an Air–Sand Interface on Gamma-ray Transport, in *NRDL-OCDM Shielding Symposium Proceedings, October 31 to November 1, 1960*, Report NP-10038, pp.301-307.
9. F. Titus, Measurement Of The Gamma-Ray Dose Near The Interface Between Two Media, *Nucl. Sci. Eng.*, 3: 609–619(1958).
10. C. E. Clifford, J. A. Carruthers, and J. R. Cunningham, γ-Radiation At Air-Ground Interfaces With Distributed Cs^{137} Sources, *Can. J. Phys.*, 38: 504–507(1960).

Chapter 2

HASL-DBM GAMMA-RAY EXPERIMENT

2.1 GENERAL METHOD

This report is a presentation of dose-rate measurements carried out at the Nevada Test Site (NTS) under the sponsorship of the Civil Effects Test Operations, Division of Biology and Medicine, USAEC. Dose rates were obtained from two point sources of different energies located on the air–ground interface. The eventual purpose is to compare these values with those expected in the case of an infinite homogeneous medium. Unfortunately the only sources both suitable and available in large enough sizes were Cs^{137} (0.662 Mev) and Co^{60} (approximately 1.25 Mev). By making measurements at the air–ground interface at source–detector distances from 10 to 900 m, we felt that the interface effect could be delineated with enough accuracy to be useful in the case of plane-distributed sources.

2.2 PHYSICAL LAYOUT

The site of the experiment was a 150-m-high microbarograph tower at NTS (Fig. 2.1). Extending from the base of the tower, a 25-m-wide by 1000-m-long area was cleared and smoothed. Distances at 10-m intervals were indicated by surveyor's stakes (Fig. 2.2). The elevation above sea level of the base of the tower and of each of the stakes was measured. The exact source location was obtained by placing it adjacent to one of the stakes.

The source-handling system is the moving point-source system described by Borella et al.[1] This system consists of a hydraulic pumping unit, plastic tubing, magnetic source-position indicators, a remote-control console, a lead shield, electrical cables, a 200-curie Co^{60} source in a single magnetic stainless-steel container, and a 300-curie Cs^{137} source in a triple magnetic stainless-steel container (Fig. 2.3).

The sources were pumped through the tubing until the appropriate magnetic locator tripped in the vicinity of the surveyor's stake, thus locating the source (Fig. 2.4).

The instrumentation package for these gamma-ray measurements was placed successively at six elevations: 0, 15, 38, 76, 114, and 148 m. The package was raised by an electrically powered winch driving an endless steel cable suspended away from the tower structure. Heights were measured with 500-ft steel tape fastened to the instrument package and to the lifting cable.

The actual source-to-detector distances were computed from simple geometric considerations. Similarly, it was thought necessary to correct for the differing source and tower-base elevations since the 10-m intervals mentioned above were actually perpendicular distances between the tower and the various source locations. Figure 2.5 illustrates this computation for the case where the source is located 700 m from the tower and the instrument package is 76 m above the ground. The line indicating ground surface represents a plot of elevations for various source locations, as measured. Hence

H is the instrument-package height above the ground
D is the distance between the source location and the tower
E is the elevation of the source location above the tower base

R is the actual source-to-detector distance
L is the actual tower base-to-source distance along the ground

The latter two values were related as follows:

$$R^2 = D^2 + (H-E)^2$$

$$L^2 = D^2 + E^2$$

In fact it was found that L and D do not differ significantly. For example, when D is 900 m and the detector is on the ground, taking E from Fig. 2.5, we see that L is greater than D by only 1 m.

2.3 INSTRUMENTATION DESCRIPTION

The gamma-ray intensities at the various locations from the cobalt and cesium sources were measured by two independent systems of instruments. The first system consisted of the well-known Victoreen condenser chamber and charger–reader combination. The lowest dose-range (largest physical size) chambers, 250 and 25 mr, were most used.

The other system consisted of the following components:

1. A chamber pressurized to 85 psig filled with a 99% argon and 1% helium mixture. This aluminum-walled ionization chamber (model RSG-3A) is manufactured by the Reuter-Stokes Corporation.

2. A vibrating capacitor electrometer, model 33c/B33c, manufactured by Electronic Instruments, Ltd., of England. This instrument was modified by the HASL Radiation Physics and Instrumentation Divisions to permit remote activation of the range, zero, input-resistor, and input-shorting controls.

3. A remote-control station built by the HASL Instrumentation Division to accomplish the remote actuation of the electrometer (Fig. 2.6).

4. A potentiometric strip-chart recorder manufactured by the Brown Instruments Division of Minneapolis-Honeywell Regulator Company.

External packaging for the instruments was designed and built by the HASL Instrumentation Division. The pressurized argon-filled chamber and the two units of the electrometer were shock-mounted in a large wood box, framed with aluminum. All electrical connections were brought to connectors accessible from the outside of the box, which was designed not to be opened except for service operations (see Fig. 2.7). The Victoreen chambers were mounted for operation within a smaller wood box containing polystyrene-foam forms, which were later replaced by shaped slabs of rubberized hair for shock protection (Fig. 2.8).

For measurements above ground level, the larger box was rigidly attached to the hoist cable of the microbarograph tower, and the smaller box was suspended from the larger box, when used (Figs. 2.9 and 2.10).

The remote-control station and the recorder were mounted on a table near the base of the tower. Electrical connections were made between the instrument package and the remote-control station with a 550-ft cable. The cable was taped at 4-ft intervals to a similar length of ½-in. rope to reduce electrical-cable tension. During operation the cable–rope combination was attached to the hoist cable with binder clips.

Atmospheric pressures and temperature ranges were measured with a standard aneroid barometer and a maximum/minimum indicating mercury thermometer, respectively.

The outputs of the cobalt and cesium gamma-ray sources were determined using Victoreen condenser chambers. These chambers were calibrated against nearly monochromatic X rays produced in the fashion described by Shambon and Murnick.[2] The sources were elevated 15 m above the ground by suspending between two poles (Fig. 2.11) the plastic tubing through which they are pumped and then locating each source in turn between two magnetic locators. The Victoreen chambers had already been elevated to a point opposite on the microbarograph tower and 10 m away; thus the exposure was made reasonably far away from scattering materials (Fig. 2.12).

2.4 INSTRUMENTATION CALIBRATION

The pressurized argon-filled chamber was calibrated separately against an Ra^{226} gamma-ray source standardized at the National Bureau of Standards. The argon-filled chamber was exposed to the cesium, radium, and cobalt sources (the first and last calibrated by HASL at the site). The three values of ionization current obtained were cesium, 1.166×10^{-12} amp/(mr/hr); radium, 1.189×10^{-12} amp/(mr/hr); and cobalt, 1.217×10^{-12} amp/(mr/hr). Because the range of these values was small, the radium value was selected as the calibration. Prior to the experiment the energy dependence of the argon-filled chamber was not determined. This is needed for the final analysis of the data.

REFERENCES

1. H. Borella, Z. Burson, and J. Jacovitch, *Evaluation of the Fallout Protection Afforded by Brookhaven National Laboratory Medical Research Center*, USAEC Report CEX-60.1, October 1961.
2. A. Shambon and D. Murnick, *Filters to Provide Nearly Monoenergetic X Rays*, USAEC Report HASL-129, New York Operations Office, July 1962.

Fig 2.1 — The 150-m microbarograph tower used to support instruments during experiment.

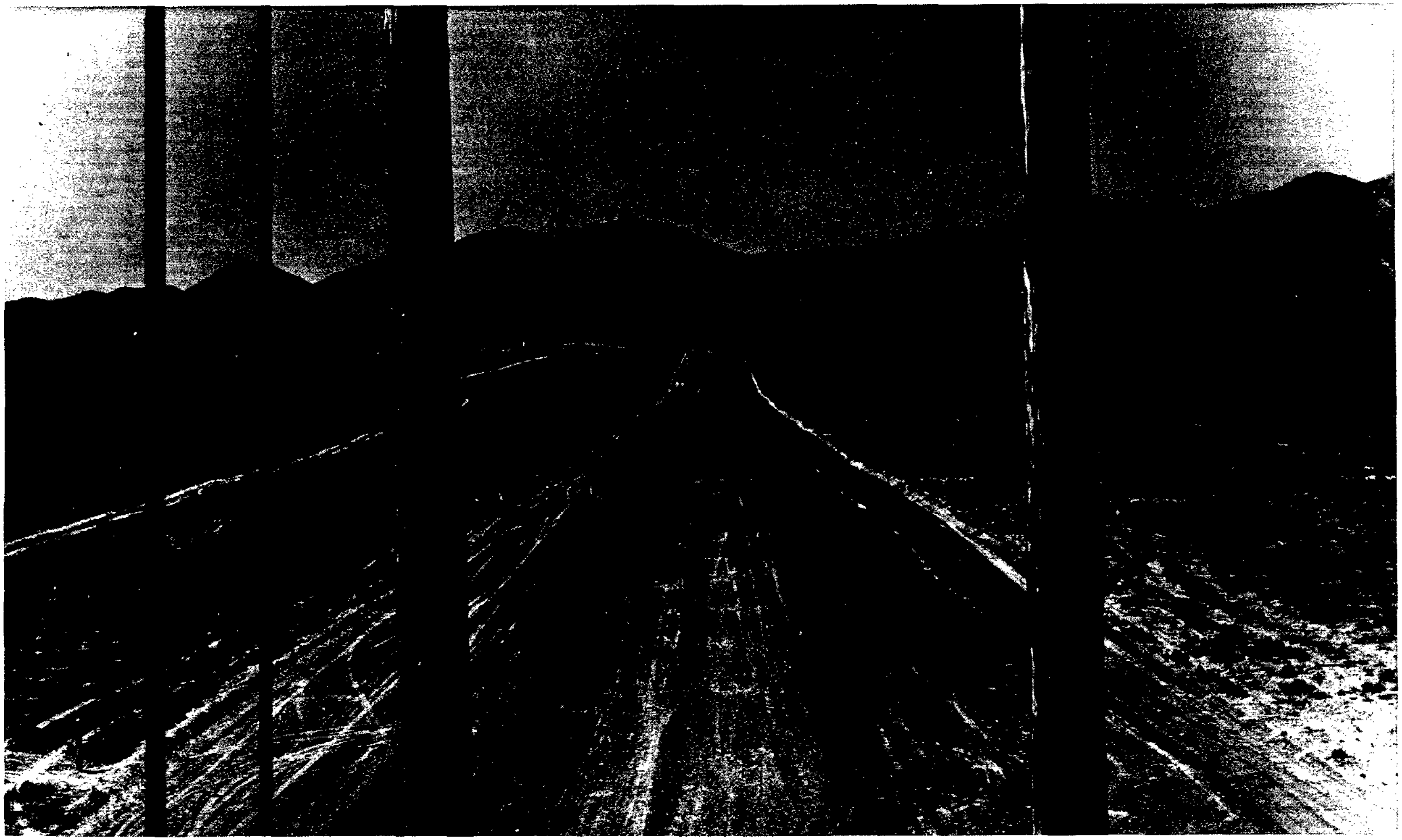

Fig. 2.2—View of 25- by 1000-m strip and surveyor's stakes. (The two telephone poles in the foreground were used to support the gamma-ray sources during calibration runs.)

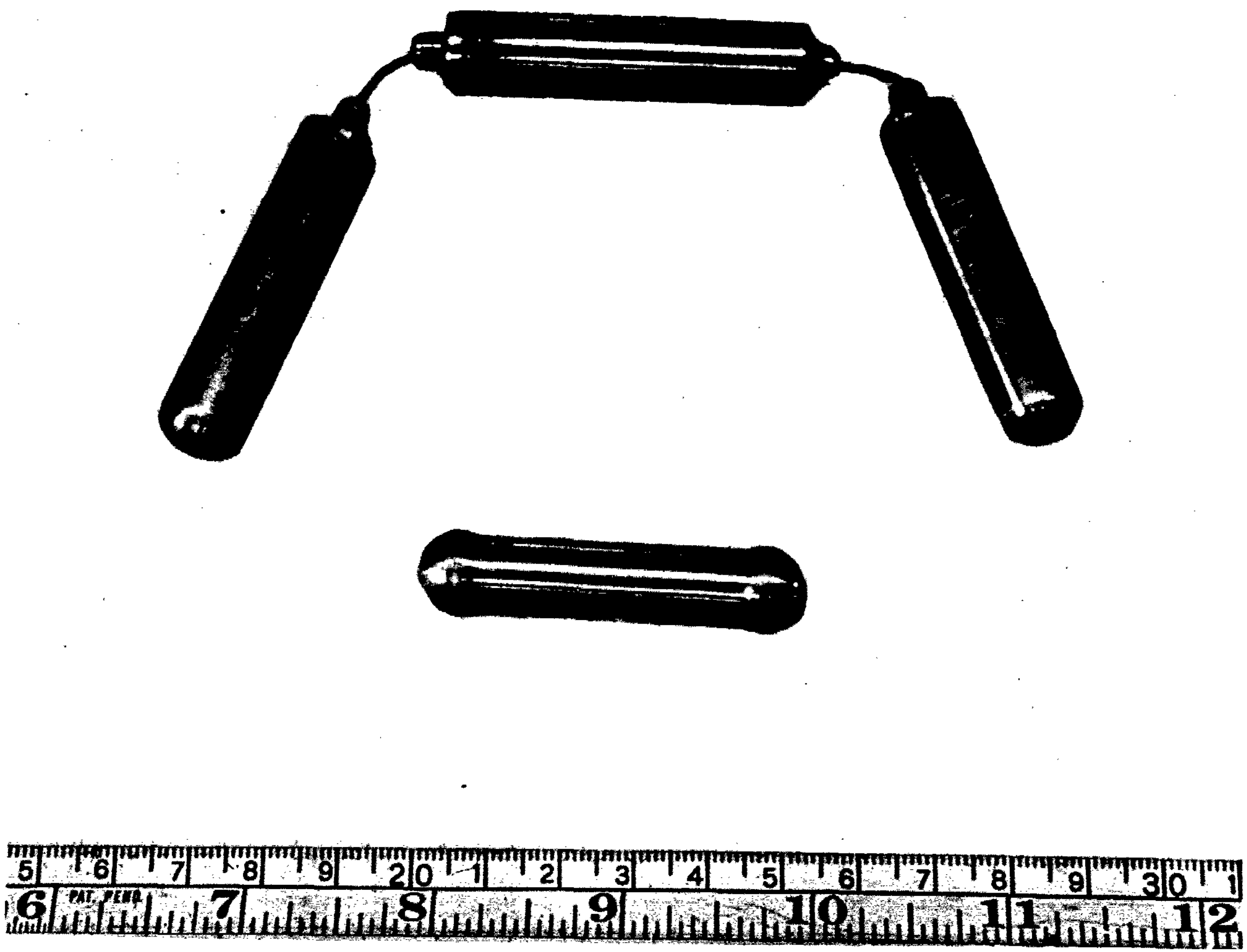

Fig. 2.3—The two gamma-ray sources. The triple capsule above is identical with the cesium source, and the single capsule, with the cobalt source.

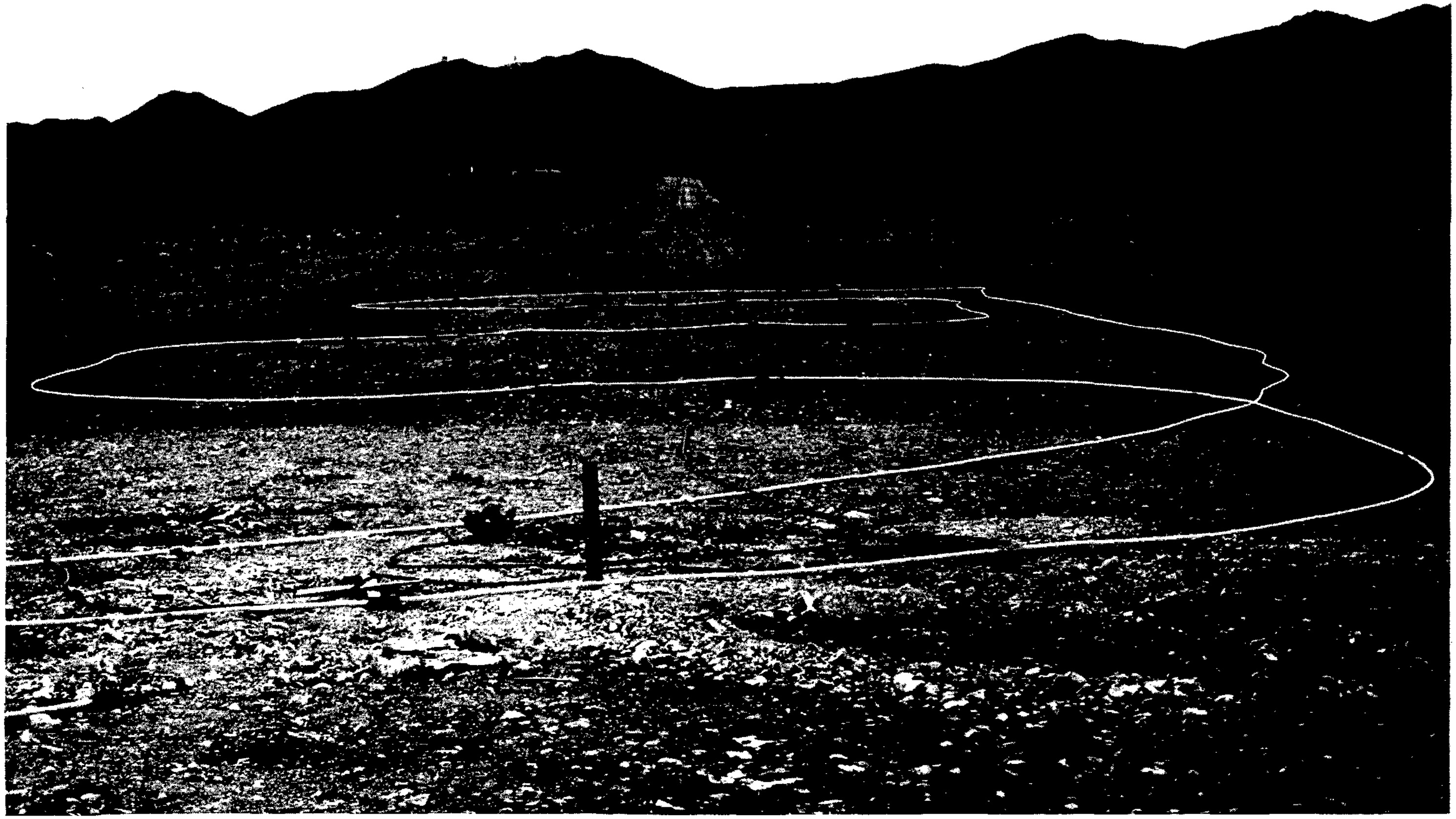

Fig. 2.4—The source tubing, surveyor's stakes, and magnetic locators. (The magnetic locators are visible as small boxes connected by black electrical cabling.)

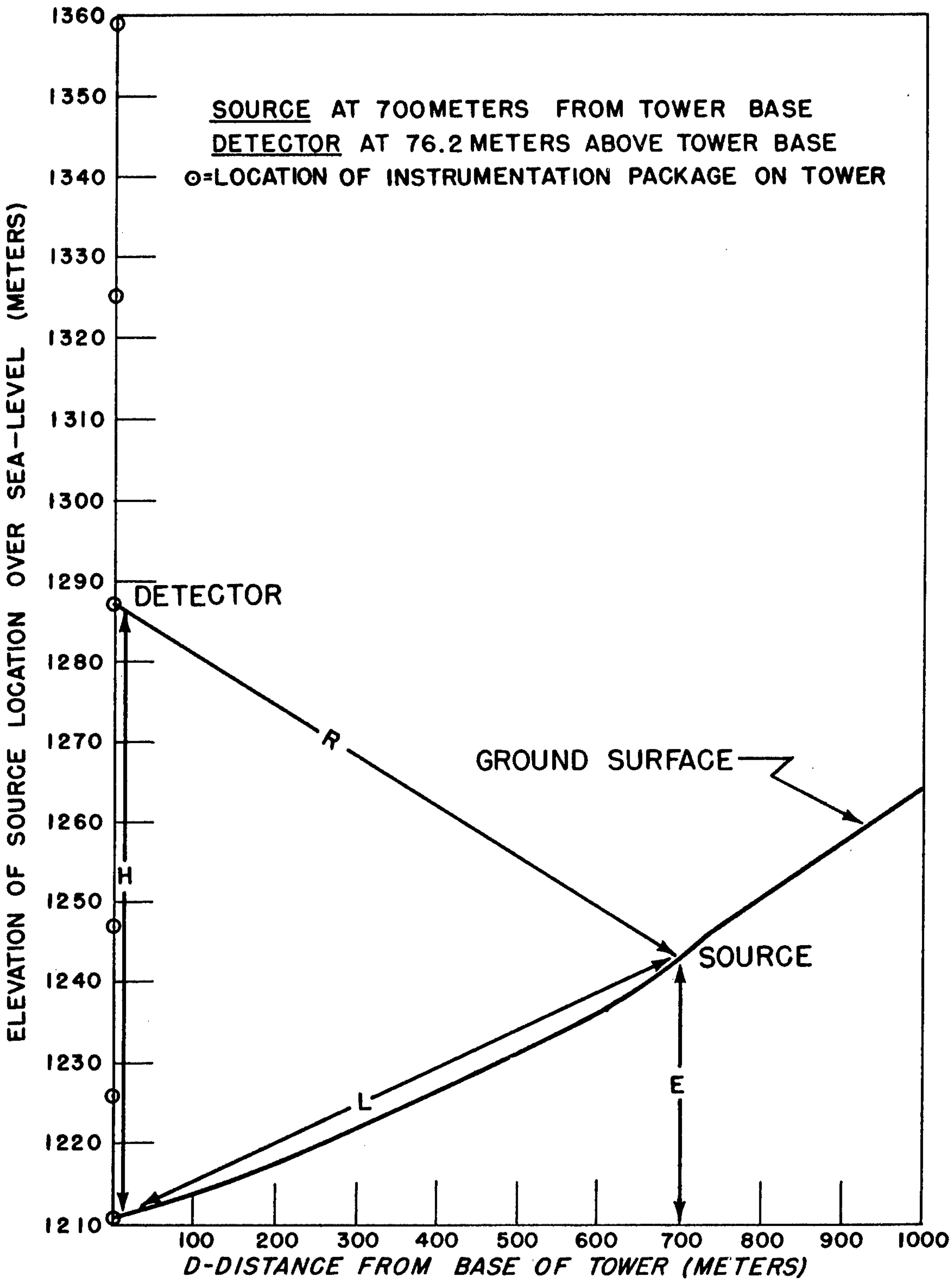

Fig. 2.5—Diagram of distances pertinent to gamma-ray experiment.

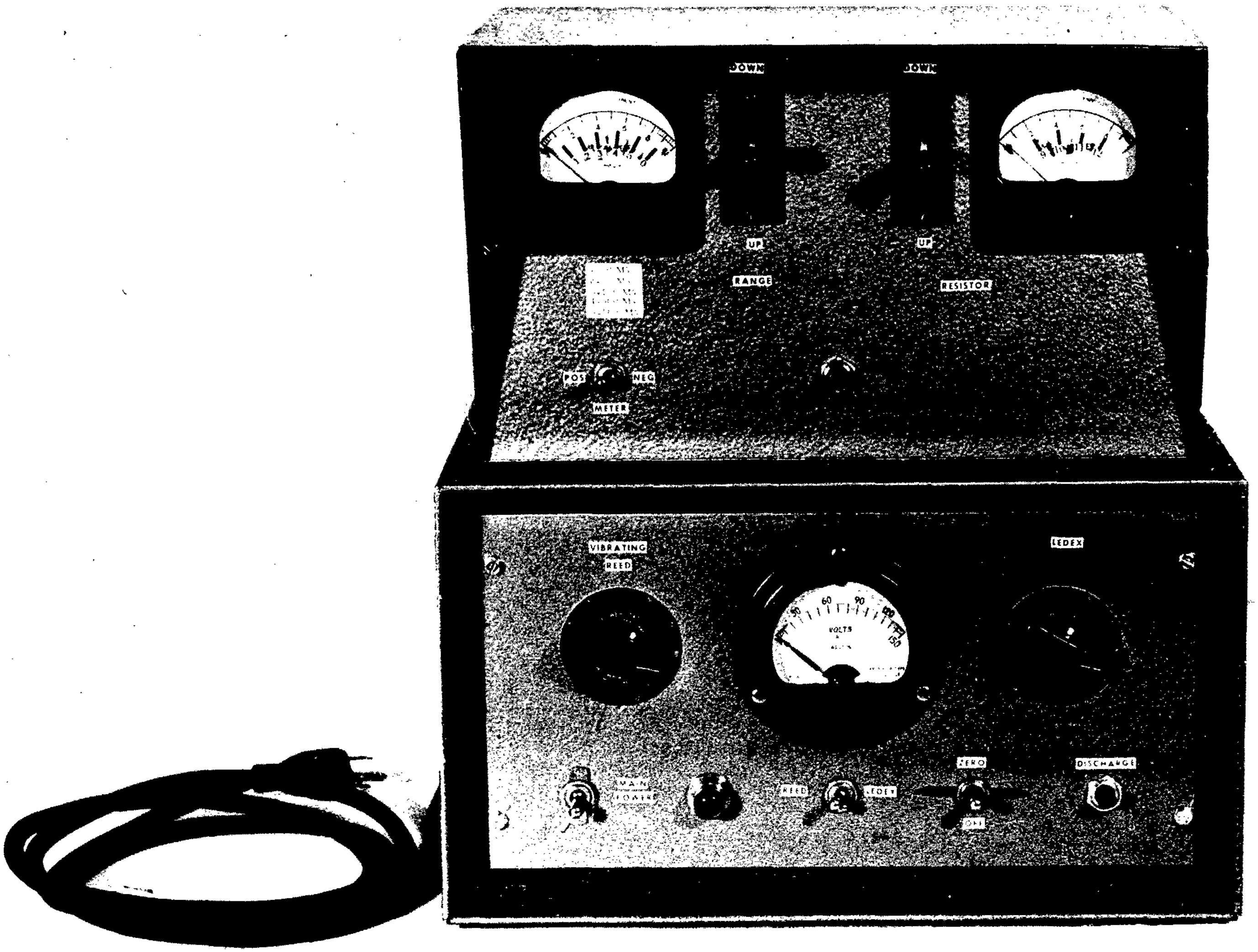

Fig. 2.6—Remote-control system for the pressurized argon-filled ionization chamber and associated electronics.

Fig. 2.7—Vibrating-capacitor electrometer and head (top 2 units), and argon-filled aluminum-walled ionization chamber (bottom cylinder).

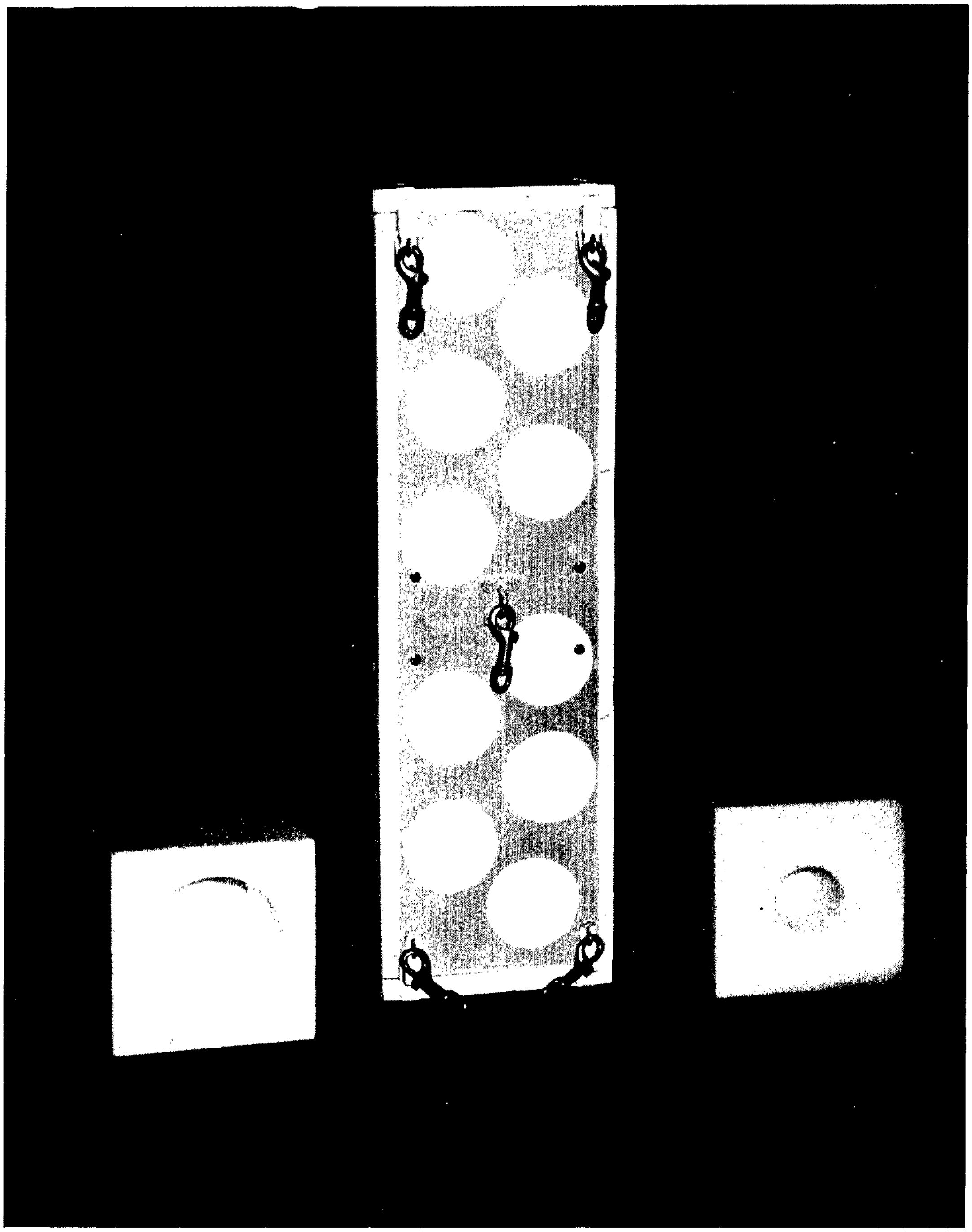

Fig. 2.8—Container for Victoreen chambers.

Fig. 2.9—Pressurized argon-filled-chamber package located on tower.

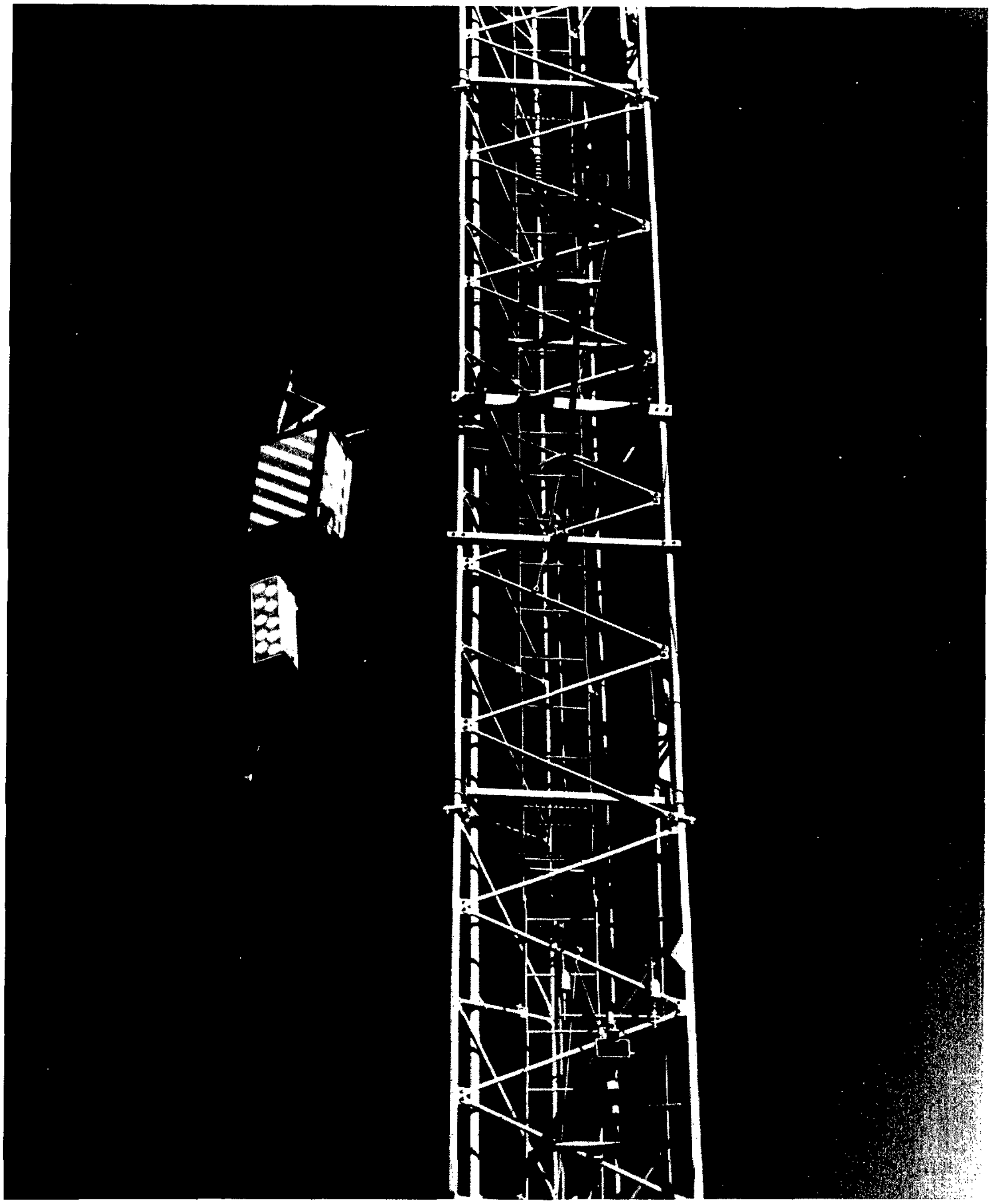

Fig. 2.10 — Argon-filled-chamber package and Victoreen chamber container suspended on the endless cable.

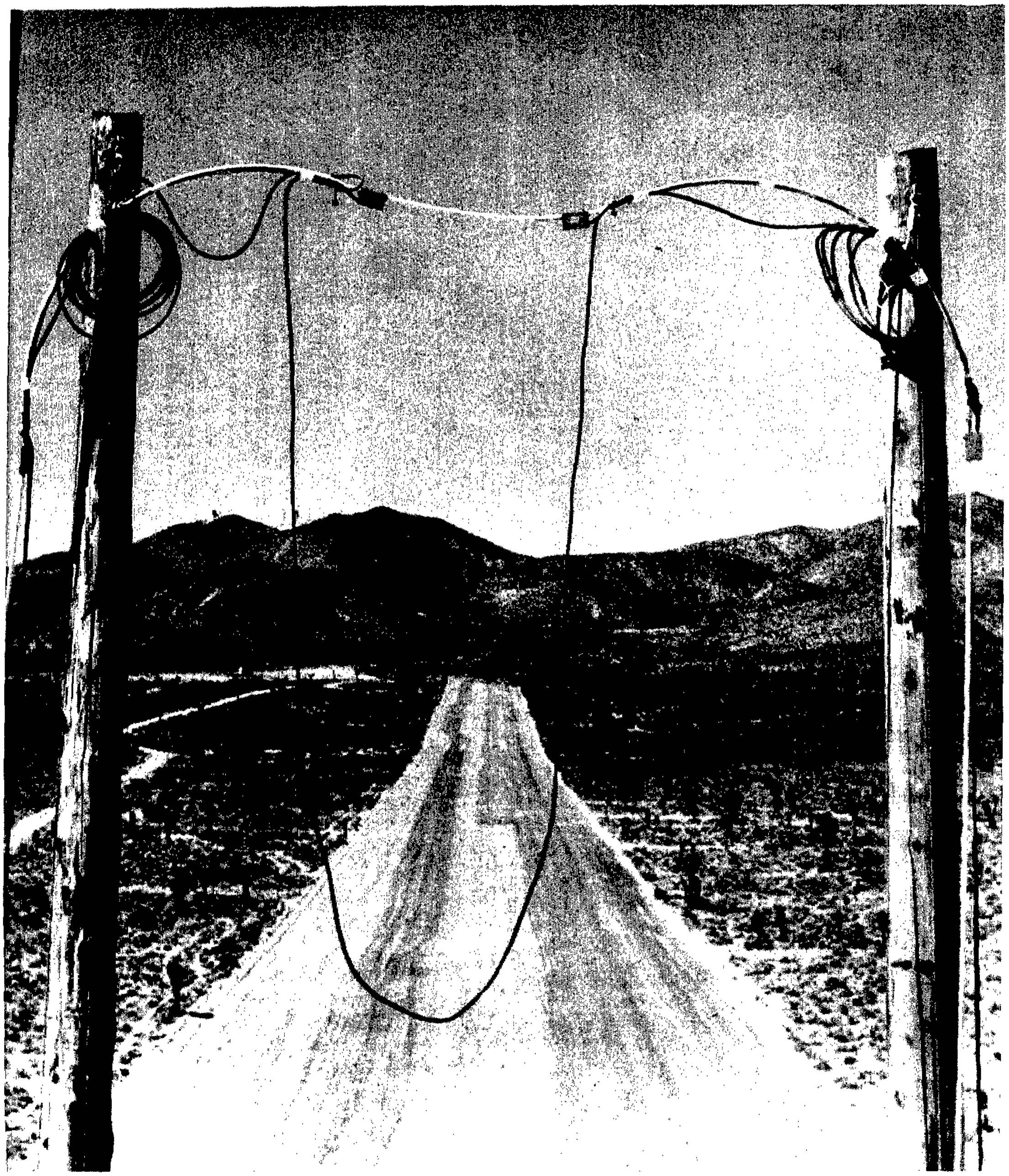

Fig. 2.11—Calibration arrangement as viewed from the tower. (The dummy source is barely visible in the plastic tubing near right-hand magnetic locator).

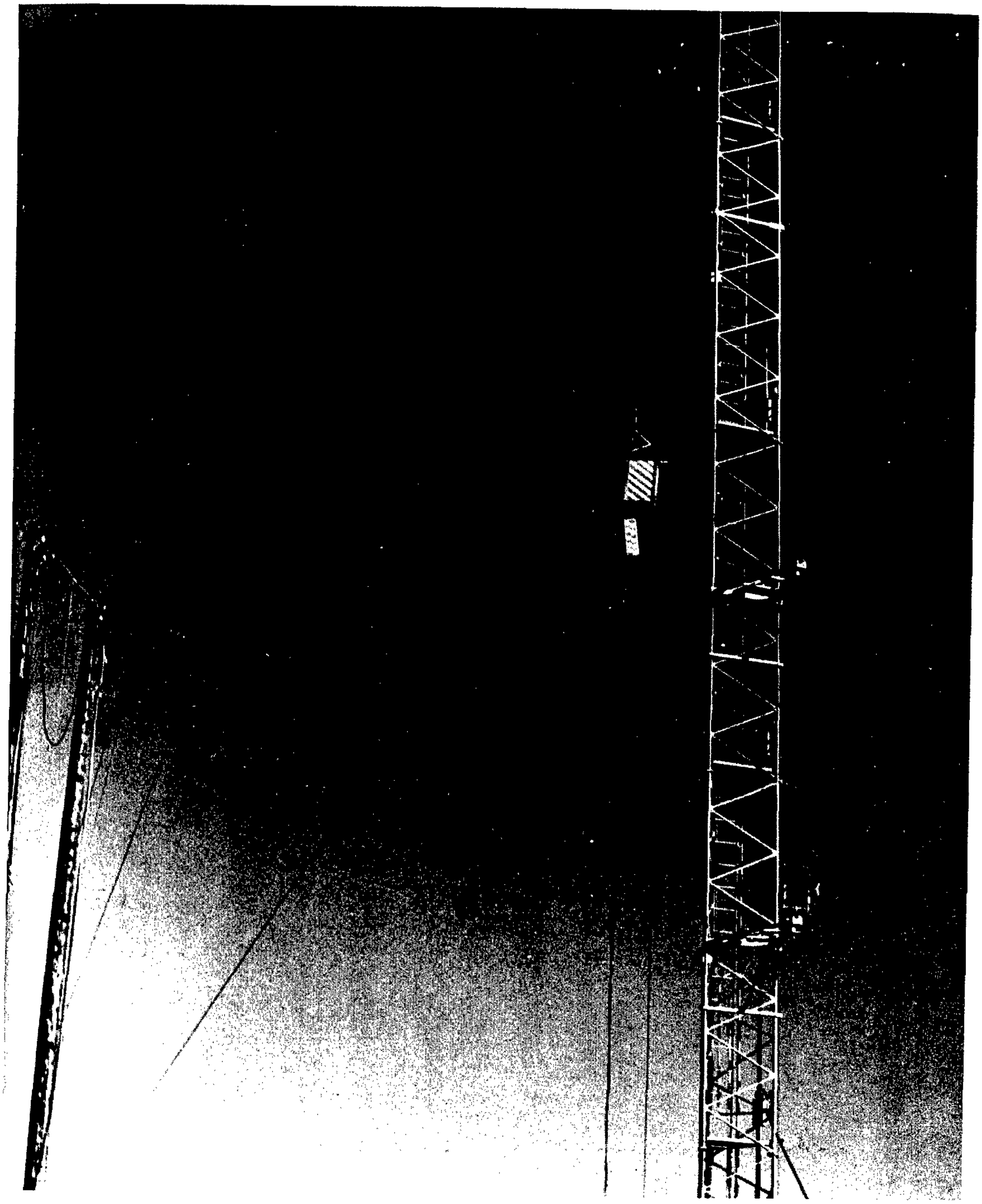

Fig. 2.12—A calibration run. Both source and detector are 15 m above the ground and separated by 10 m.

Chapter 3

PRESENTATION OF DATA

3.1 GENERAL RESULTS

The measurements shown in Tables 3.1 and 3.2 and in Figs. 3.1 to 3.4 exhibit two noteworthy characteristics. First, the dose-rate values increase with increasing instrument height above ground to a given maximum and then decrease. The maximum dose-rate values occur at greater instrument heights as the tower-to-source distance increases. This is consonant with the behavior mentioned earlier which was observed during the weapons tests.[1,2] Second, the condenser-chamber values are always less than those obtained at the same locations with the pressurized argon-filled chamber. This indicates the need for a detailed analysis of the argon-filled chamber energy dependence. When this response is determined, the infinite-medium response can also be determined, and eventually the effect of the interface.

3.2 SUMMARY OF PRELIMINARY DATA ANALYSIS

In Table 3.3 the data are exhibited in a different fashion. Here dose rates are expressed as

$$S(H,L) = IR^2$$

wnere I is the dose rate in milliroentgens per hour and R is the source–detector distance.

If the source calibration S is expressed in units of milliroentgens per hour at 1 meter, then the dose resulting from the uncollided photon flux, in terms of milliroentgens square meters per hour, is $S(R) = Se^{-\mu R}$. The buildup factor, which is the ratio of the dose from the uncollided photon flux to the dose from the total flux, is therefore

$$B(H,L) = \frac{S(H,L)}{Se^{-\mu R}}$$

B(H,L) is the buildup factor appearing in Table 3.3. The cross section μ is taken from Grodstein.[3] The average of many air-density measurements taken at the tower base was in close agreement with standard table values for dry, summer air.[4] Hence the tabular air-density value for the elevation in question was employed. The value of S is the source calibration referred to above in units of milliroentgens per hour at 1 meter.

The effect of the interface on gamma-ray measurements has customarily been given as a correction factor that expresses the change in dose compared to that which would prevail in an infinite homogeneous medium with the same source–detector distance.[5–7] Once the energy response of the argon-filled chamber has been obtained, it will be possible to compute its infinite-homogeneous-medium response. The correction factor is defined as

$$K(H,L) = \frac{I(H,L)}{I(R)}$$

where I(H,L) is the dose rate measured at a height H above the interface and a distance L along the interface from the source and I(R) is the dose rate calculated from homogeneous theory. As shown above,

$$I(H,L) = \frac{S(H,L)}{R^2} = \frac{Se^{-\mu R}}{R^2} B(H,L)$$

and by definition

$$I(R) = \frac{Se^{-\mu R}}{R^2} B(R)$$

where B(R) is the buildup factor obtained for the infinite homogeneous medium. Therefore

$$K(H,L) = \frac{B(H,L)}{B(R)}$$

3.3 CONCLUSION

This report presents data resulting from a reasonably well controlled experiment on the propagation of gamma rays along or near the air–ground interface. These data will enable us, and perhaps others, to infer interface-effect values for various source–detector configurations for cases of cobalt and cesium gamma rays.

REFERENCES

1. A. J. Breslin and L. R. Solon, *Fallout Countermeasures For AEC Facilities*, USAEC Report NYO-4682-A, New York Operations Office, December 1955.
2. R. T. Graveson, *Radiation Protection Within a Standard Housing Structure*, USAEC Report NYO-4714, New York Operations Office, November 1956.
3. Gladys W. Grodstein, X-Ray Attenuation Coefficients From 10 KeV to 100 MeV, *Nat. Bur. Std. (U.S.), Circ. 583* (Apr. 30, 1957).
4. L. L. Beranek, Acoustic Properties of Gases, in *American Institute of Physics Handbook,* Dwight E. Gray (Ed.), McGraw-Hill Book Company, Inc., New York, 1957.
5. M. J. Berger, Calculation Of Energy Dissipation by γ-Radiation Near the Interface Between Two Media, *J. Appl. Phys.*, 28: 1502–1508 (December 1957).
6. F. Titus, Measurement of the Gamma-Ray Dose Near the Interface Between Two Media, *Nucl. Sci. Eng.*, 3: 609–619 (1958).
7. C. E. Clifford, J. A. Carruthers, and J. R. Cunningham, γ-Radiation At Air-Ground Interfaces With Distributed Cs^{137} Sources, *Can. J. Phys.*, 38: 504–507 (1960).

TABLE 3.1—CESIUM GAMMA-RAY DOSE RATES INFERRED FROM ARGON-FILLED-CHAMBER AND CONDENSER-CHAMBER MEASUREMENTS
(Cesium source, 95.74 r/hr at 1 m)

Height of detector, m	Source distance from tower, m															
	10	20	30	40	60	80	100	120	200	300	400	500	600	700	800	900
0		254.0		57.51	26.89	14.99	8.56	5.78	0.981	0.313	0.136	0.0486	0.0175	0.00618	0.00378	0.000757
15.24	340.62			68.96	33.64	18.17	11.05	7.23	1.83	0.491	0.167	0.0597	0.0252	0.00589	0.00379	0.00177
	234.08*				27.04*											
38.1	78.2	65.6		40.4	26.35	16.90	10.93	7.57	1.94	0.582	0.197	0.0729	0.0324	0.0122	0.00391	0.00114
	69.32*				19.88*											
76.2	20.94			17.28	13.76	10.75	8.17	6.23	1.94	0.641	0.225	0.0841	0.0366	0.0143	0.00580	0.00252
	17.02*				10.77*											
114.3	9.46			8.83	7.70	6.51	5.38	4.54	1.82	0.670	0.231	0.0899	0.0382	0.0197	0.00706	0.00353
	6.93*				5.81*											
148.4	5.47			5.30	4.39	3.94	3.37	2.89	1.85	0.634	0.228	0.0902	0.0387	0.0156	0.00656	0.00404

*Condenser-chamber measurements.

TABLE 3.2—COBALT GAMMA-RAY DOSE RATES INFERRED FROM ARGON-FILLED-CHAMBER AND CONDENSER-CHAMBER MEASUREMENTS
(Cobalt source, 253.40 r/hr at 1 m)

Height of detector, m	Source distance from tower, m															
	10	20	30	40	60	80	100	120	200	300	400	500	600	700	800	900
0		620	275	136	64.1	35.5	21.8	14.5	1.85	0.649	0.428	0.222	0.0682	0.0326	0.0167	0.00833
15.24	838.00	463	279	172	80.0	45.5	27.5	17.8	4.85	1.41	0.523	0.206	0.0965	0.0431	0.0216	0.0111
					69.6*			15.8*								
38.1	192	159	126	95.9	60.8	39.5	26.2	18.1	5.30	1.60	0.578	0.242	0.108	0.0526	0.0223	0.0105
	175*			74.4*	52.4*			15.2*								
76.2	48.4	47.3	44.6	40.0	30.7	23.4	18.0	14.1	5.14	1.74	0.664	0.277	0.128	0.0609	0.0294	0.0191
					27.9*											
114.3	19.8	19.8	19.6	18.9	16.9	14.4	11.9	9.74	4.43	1.67	0.679	0.273	0.138	0.0631	0.0278	0.0160
	17.5*				15.3*											
148.4	11.7	12.1	12.0	11.7	10.7	9.59	8.35	7.12	3.69	1.50	0.652	0.291	0.137	0.0661	0.0301	0.0170
	9.48*															

*Condenser-chamber measurements.

TABLE 3.3 — ARGON-FILLED PRESSURE-CHAMBER RESULTS

Distance from tower base: Meters	Distance from tower base: Mean free paths	Source–detector distance, mean free paths	Dose, mr m^2/hr	Buildup factor
Cobalt source, 253.40 r/hr at 1 m; elevation, 0.000 m or 0.000 mean free path				
20	0.121	0.121	2.482E + 05	1.10
30	0.182	0.182	2.477E + 05	1.17
40	0.243	0.243	2.178E + 05	1.09
60	0.364	0.364	2.309E + 05	1.31
80	0.486	0.486	2.274E + 05	1.45
100	0.608	0.608	2.182E + 05	1.58
120	0.729	0.729	2.090E + 05	1.71
200	1.216	1.216	7.409E + 04	0.98
300	1.824	1.824	5.849E + 04	1.43
400	2.432	2.432	6.858E + 04	3.08
500	3.040	3.040	5.558E + 04	4.58
600	3.648	3.648	2.459E + 04	3.73
700	4.257	4.257	1.600E + 04	4.46
800	4.866	4.866	1.071E + 04	5.49
901	5.475	5.475	6.764E + 03	6.37
Cobalt source, 253.40 r/hr at 1 m; elevation, 15.240 m or 0.092 mean free path				
10	0.060	0.109	2.715E + 05	1.19
20	0.121	0.150	2.838E + 05	1.30
30	0.182	0.201	3.079E + 05	1.48
40	0.243	0.257	3.088E + 05	1.57
60	0.364	0.373	3.021E + 05	1.73
80	0.486	0.491	2.983E + 05	1.92
100	0.608	0.611	2.787E + 05	2.02
120	0.729	0.732	2.584E + 05	2.12
200	1.216	1.216	1.943E + 05	2.58
300	1.824	1.823	1.269E + 05	3.10
400	2.432	2.430	8.368E + 04	3.75
500	3.040	3.038	5.150E + 04	4.24
600	3.648	3.646	3.474E + 04	5.25
700	4.257	4.254	2.113E + 04	5.87
800	4.866	4.863	1.383E + 04	7.06
901	5.475	5.471	9.001E + 03	8.45
Cobalt source, 253.40 r/hr at 1 m; elevation, 38.100 m or 0.231 mean free path				
10	0.060	0.237	2.939E + 05	1.47
20	0.121	0.258	2.867E + 05	1.46
30	0.182	0.290	2.871E + 05	1.51
40	0.243	0.330	2.836E + 05	1.55
60	0.364	0.425	2.984E + 05	1.80
80	0.486	0.531	3.021E + 05	2.02
100	0.608	0.642	2.932E + 05	2.20
120	0.729	0.757	2.812E + 05	2.36
200	1.216	1.229	2.170E + 05	2.93
300	1.824	1.830	1.451E + 05	3.57

TABLE 3.3 — (Continued)

Distance from tower base: Meters	Distance from tower base: Mean free paths	Source–detector distance, mean free paths	Dose, mr m^2/hr	Buildup factor
	Cobalt source, 253.40 r/hr at 1 m; elevation, 38.100 m or 0.231 mean free path			
400	2.432	2.434	9.277E + 04	4.17
500	3.040	3.040	6.057E + 04	4.99
600	3.648	3.646	3.889E + 04	5.88
700	4.257	4.253	2.577E + 04	7.15
800	4.866	4.860	1.427E + 04	7.27
901	5.475	5.468	8.505E + 03	7.96
	Cobalt source, 253.40 r/hr at 1 m; elevation, 76.200 m or 0.463 mean free path			
10	0.060	0.465	2.838E + 05	1.78
20	0.121	0.474	2.889E + 05	1.83
30	0.182	0.490	2.906E + 05	1.87
60	0.364	0.580	2.799E + 05	1.97
80	0.486	0.659	2.760E + 05	2.10
100	0.608	0.750	2.748E + 05	2.29
120	0.729	0.849	2.757E + 05	2.54
200	1.216	1.285	2.301E + 05	3.28
300	1.824	1.865	1.639E + 05	4.17
400	2.432	2.458	1.086E + 05	5.01
500	3.040	3.057	7.012E + 04	5.88
600	3.648	3.658	4.641E + 04	7.11
700	4.257	4.261	2.995E + 04	8.38
800	4.866	4.866	1.885E + 04	9.66
901	5.475	5.471	1.548E + 04	14.53
	Cobalt source, 253.40 r/hr at 1 m; elevation, 114.300 m or 0.694 mean free path			
10	0.060	0.695	2.594E + 05	2.05
20	0.121	0.701	2.637E + 05	2.09
30	0.182	0.712	2.693E + 05	2.16
40	0.243	0.728	2.717E + 05	2.22
60	0.364	0.774	2.742E + 05	2.34
80	0.486	0.834	2.713E + 05	2.46
100	0.608	0.906	2.648E + 05	2.58
120	0.729	0.988	2.579E + 05	2.73
200	1.216	1.378	2.280E + 05	3.57
300	1.824	1.927	1.680E + 05	4.55
400	2.432	2.503	1.152E + 05	5.56
500	3.040	3.091	7.067E + 04	6.13
600	3.648	3.685	5.077E + 04	7.99
700	4.257	4.282	3.134E + 04	8.95
800	4.866	4.882	1.794E + 04	9.34
901	5.475	5.484	1.303E + 04	12.39

TABLE 3.3— (Continued)

Distance from tower base: Meters	Distance from tower base: Mean free paths	Source–detector distance, mean free paths	Dose, mr m^2/hr	Buildup factor
Cobalt source, 253.40 r/hr at 1 m; elevation, 148.400 m or 0.901 mean free path				
10	0.060	0.902	2.578E + 05	2.50
20	0.121	0.906	2.690E + 05	2.62
40	0.243	0.926	2.720E + 05	2.71
60	0.364	0.961	2.681E + 05	2.76
80	0.486	1.009	2.648E + 05	2.86
100	0.608	1.069	2.585E + 05	2.97
120	0.729	1.139	2.501E + 05	3.08
200	1.216	1.487	2.212E + 05	3.86
300	1.824	2.004	1.632E + 05	4.77
400	2.432	2.561	1.158E + 05	5.92
500	3.040	3.136	7.754E + 04	7.04
600	3.648	3.721	5.140E + 04	8.38
700	4.257	4.311	3.328E + 04	9.79
800	4.866	4.905	1.962E + 04	10.46
901	5.475	5.503	1.394E + 04	13.52
Cesium source, 95.74 r/hr at 1 m; elevation, 0.000 m or 0.000 mean free path				
20	0.164	0.164	1.017E + 05	1.25
40	0.328	0.328	9.208E + 04	1.33
60	0.493	0.493	9.693E + 04	1.65
80	0.657	0.657	9.611E + 04	1.93
100	0.822	0.822	8.571E + 04	2.03
120	0.986	0.986	8.334E + 04	2.33
200	1.644	1.644	3.928E + 04	2.12
300	2.466	2.466	2.820E + 04	3.47
400	3.289	3.289	2.179E + 04	6.10
500	4.111	4.111	1.216E + 04	7.75
600	4.934	4.934	6.311E + 03	9.16
700	5.757	5.757	3.034E + 03	10.03
800	6.581	6.581	2.425E + 03	18.27
901	7.404	7.404	6.147E + 02	10.55
Cesium source, 95.74 r/hr at 1 m; elevation, 15.240 m or 0.125 mean free path				
10	0.082	0.147	1.105E + 05	1.33
40	0.328	0.348	1.239E + 05	1.83
60	0.493	0.504	1.269E + 05	2.19
80	0.657	0.665	1.193E + 05	2.42
100	0.822	0.827	1.125E + 05	2.68
120	0.986	0.990	1.049E + 05	2.95
200	1.644	1.644	7.332E + 04	3.96
300	2.466	2.465	4.419E + 04	5.43
400	3.289	3.286	2.672E + 04	7.46
500	4.111	4.108	1.492E + 04	9.48
600	4.934	4.930	9.074E + 03	13.12
700	5.757	5.753	2.887E + 03	9.50
800	6.581	6.576	2.427E + 03	18.20
901	7.404	7.399	1.435E + 03	24.50

TABLE 3.3 — (Continued)

Distance from tower base: Meters	Distance from tower base: Mean free paths	Source–detector distance, mean free paths	Dose, mr m^2/hr	Buildup factor
Cesium source, 95.74 r/hr at 1 m; elevation, 38.100 m or 0.313 mean free path				
10	0.082	0.321	1.197E + 05	1.72
20	0.164	0.348	1.182E + 05	1.75
40	0.328	0.446	1.195E + 05	1.95
60	0.493	0.575	1.295E + 05	2.40
80	0.657	0.718	1.292E + 05	2.77
120	0.986	1.024	1.176E + 05	3.42
200	1.644	1.662	7.946E + 04	4.37
300	2.466	2.474	5.279E + 04	6.55
400	3.289	3.291	3.162E + 04	8.88
500	4.111	4.110	1.824E + 04	11.62
600	4.934	4.931	1.166E + 04	16.88
700	5.757	5.751	5.978E + 03	19.65
800	6.581	6.573	2.502E + 03	18.70
901	7.404	7.395	9.234E + 02	15.70
Cesium source, 95.74 r/hr at 1 m; elevation, 76.200 m or 0.626 mean free path				
10	0.082	0.629	1.225E + 05	2.40
40	0.328	0.698	1.248E + 05	2.62
60	0.493	0.784	1.258E + 05	2.88
80	0.657	0.892	1.274E + 05	3.24
100	0.822	1.015	1.247E + 05	3.59
120	0.986	1.149	1.218E + 05	4.01
200	1.644	1.738	8.685E + 04	5.16
300	2.466	2.522	6.039E + 04	7.85
400	3.289	3.324	3.683E + 04	10.68
500	4.111	4.134	2.129E + 04	13.88
600	4.934	4.947	1.327E + 03	1.95
700	5.757	5.762	7.034E + 03	23.38
800	6.581	6.580	3.719E + 03	28.00
901	7.404	7.399	2.043E + 03	34.88
Cesium source, 95.74 r/hr at 1 m; elevation, 114.300 m or 0.939 mean free path				
10	0.082	0.940	1.239E + 05	3.31
40	0.328	0.985	1.269E + 05	3.55
60	0.493	1.046	1.249E + 05	3.71
80	0.657	1.127	1.226E + 05	3.95
100	0.822	1.225	1.197E + 05	4.26
120	0.986	1.337	1.202E + 05	4.78
200	1.644	1.864	9.370E + 04	6.31
300	2.466	2.606	6.741E + 04	9.53
400	3.289	3.385	3.921E + 04	12.09
500	4.111	4.180	2.327E + 04	15.90
600	4.934	4.984	1.405E + 04	21.44
700	5.757	5.790	9.785E + 03	33.45
800	6.581	6.602	4.558E + 03	35.07
901	7.404	7.416	2.875E + 03	49.93

TABLE 3.3 — (Continued)

Distance from tower base: Meters	Distance from tower base: Mean free paths	Source–detector distance, mean free paths	Dose, mr m^2/hr	Buildup factor
Cesium source, 95.74 r/hr at 1 m; elevation, 148.400 m or 1.219 mean free paths				
10	0.082	1.219	1.205E + 05	4.26
40	0.328	1.252	1.232E + 05	4.50
60	0.493	1.300	1.099E + 05	4.21
80	0.657	1.365	1.088E + 05	4.45
100	0.822	1.445	1.043E + 05	4.62
120	0.986	1.540	1.015E + 05	4.94
200	1.644	2.011	1.109E + 05	8.66
300	2.466	2.710	6.898E + 04	10.83
400	3.289	3.463	4.051E + 04	13.51
500	4.111	4.241	2.403E + 04	17.45
600	4.934	5.032	1.452E + 04	23.26
700	5.757	5.830	7.854E + 03	27.92
800	6.581	6.634	4.276E + 03	33.97
901	7.404	7.442	3.314E + 03	59.10

TABLE 3.4 — VICTOREEN CONDENSER CHAMBERS

Distance from tower base: Meters	Distance from tower base: Mean free paths	Source–detector distance, mean free paths	Dose, mr m^2/hr	Buildup factor	Elevation: Meters	Elevation: Mean free paths
Cobalt source, 253.40 r/hr at 1 m						
60	0.364	0.373	2.629E + 05	1.50	15.240	0.092
120	0.729	0.732	2.293E + 05	1.88	15.240	0.092
10	0.060	0.237	2.694E + 05	1.34	38.100	0.231
40	0.243	0.330	2.200E + 05	1.20	38.100	0.231
60	0.364	0.425	2.572E + 05	1.55	38.100	0.231
120	0.729	0.757	2.361E + 05	1.98	38.100	0.231
60	0.364	0.580	2.543E + 05	1.79	76.200	0.463
10	0.060	0.695	2.292E + 05	1.81	114.300	0.694
60	0.364	0.774	2.483E + 05	2.12	114.300	0.694
10	0.060	0.902	2.089E + 05	2.03	148.400	0.901
Cesium source, 95.74 r/hr at 1 m						
10	0.082	0.082	8.756E + 04	0.99	0.000	0.000
10	0.082	0.147	7.583E + 04	0.91	15.240	0.125
60	0.493	0.504	0.019E + 05	1.76	15.240	0.125
10	0.082	0.321	0.061E + 05	1.52	38.100	0.313
60	0.493	0.575	9.768E + 04	1.81	38.100	0.313
10	0.082	0.629	9.971E + 04	1.95	76.200	0.626
60	0.493	0.784	9.846E + 04	2.25	76.200	0.626
10	0.082	0.940	9.080E + 04	2.42	114.300	0.939
60	0.493	1.046	9.429E + 04	2.80	114.300	0.939

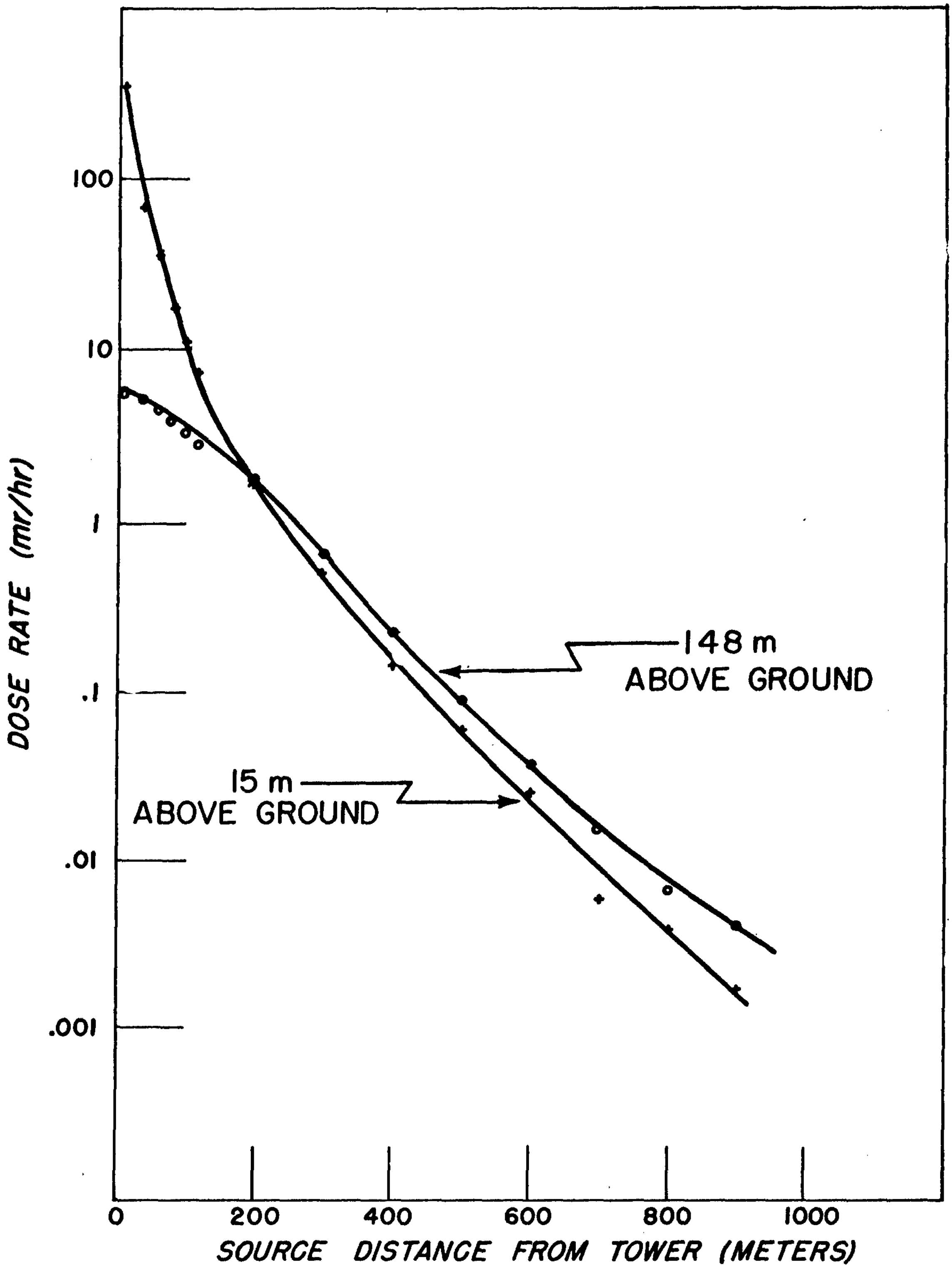

Fig. 3.1—Argon-filled-chamber measurements of Cs^{137} gamma rays.

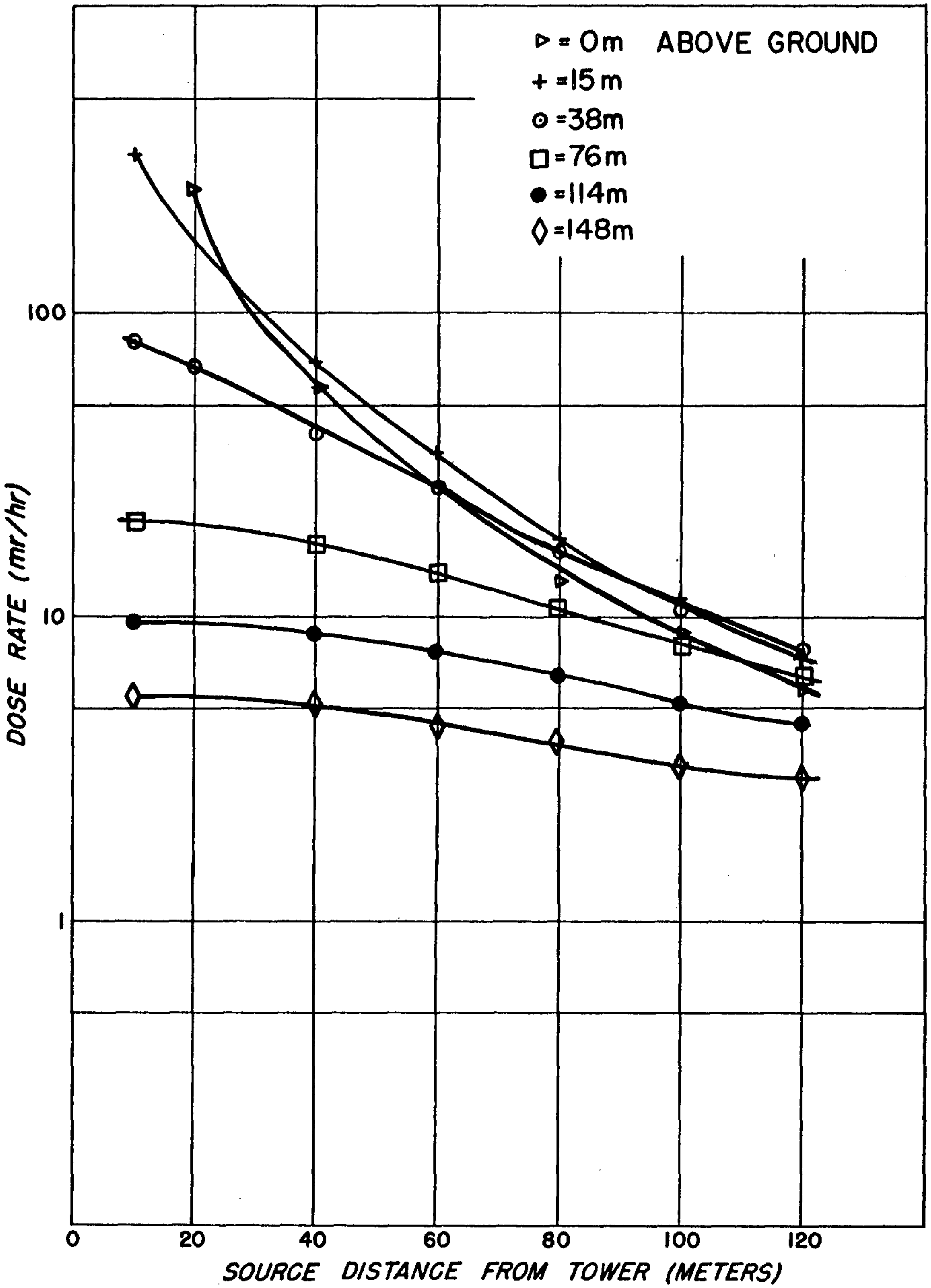

Fig. 3.2—Argon-filled-chamber measurements of Cs^{137} gamma rays.

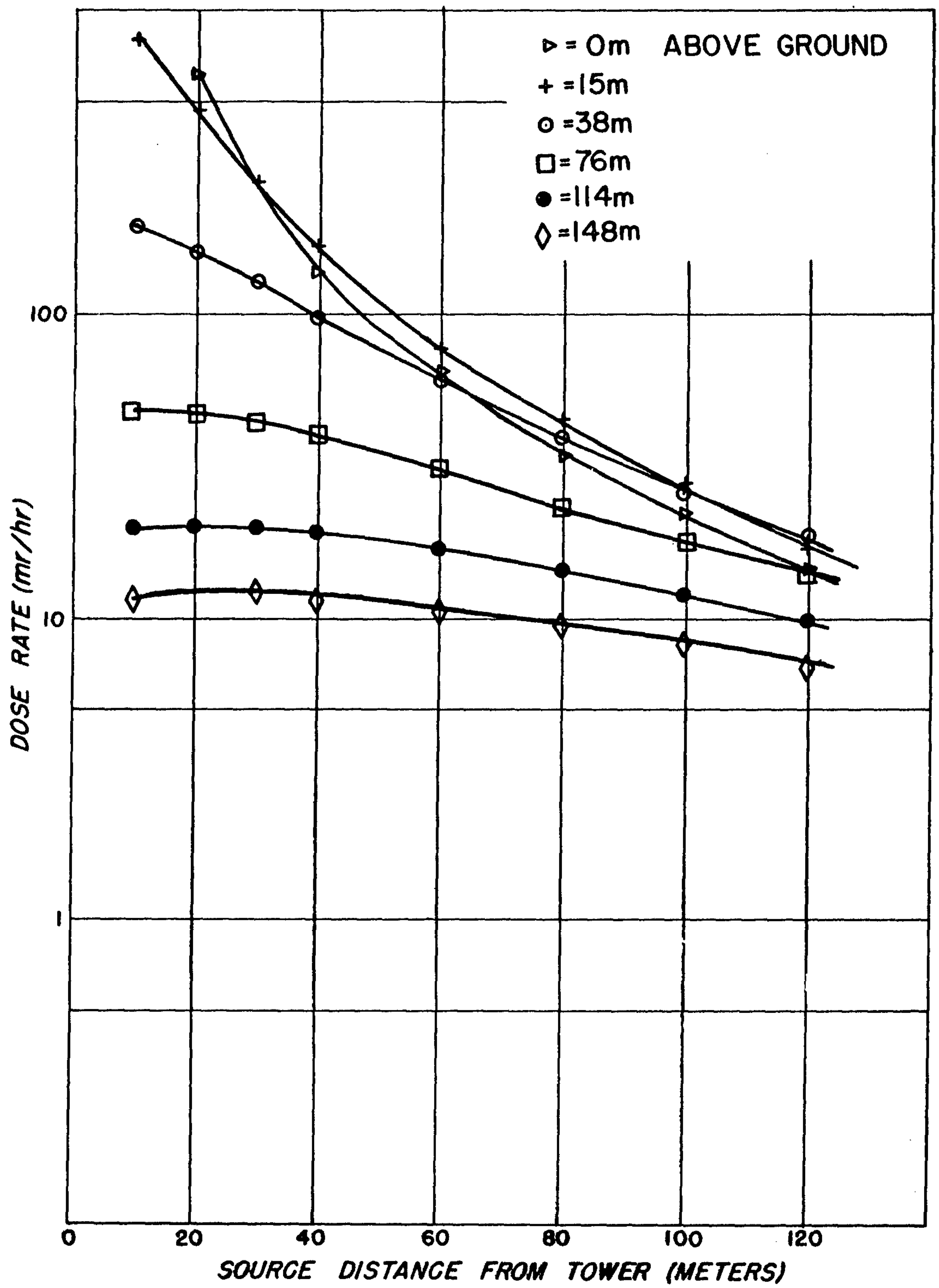

Fig. 3.3—Argon-filled-chamber measurements of Co^{60} gamma rays.

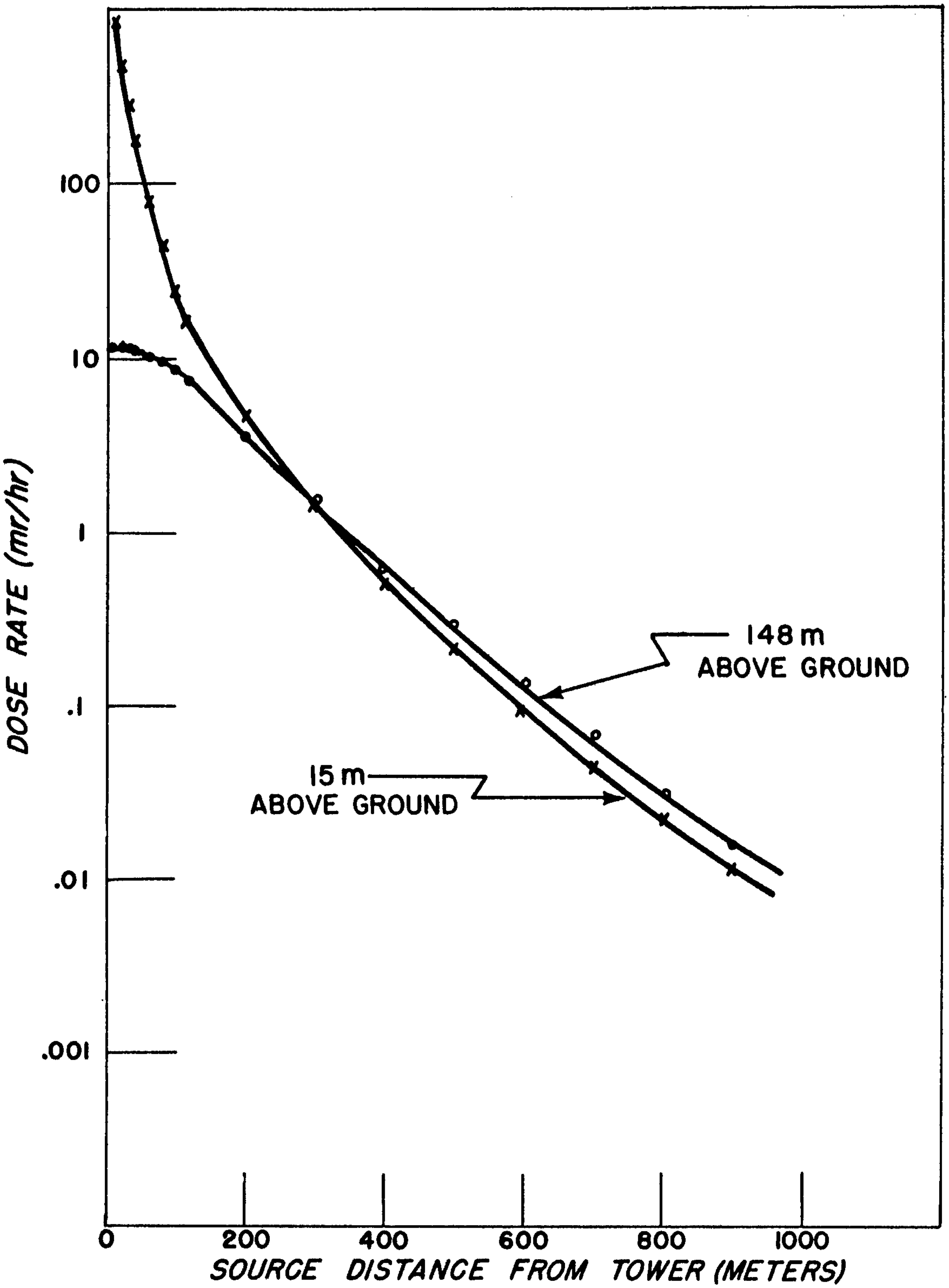

Fig. 3.4—Argon-filled-chamber measurements of Co^{60} gamma rays.